

# Quantum State Transfer via a Multimode Resonator

Yang He<sup>1,2</sup> and Yu-Xiang Zhang<sup>1,2,3,\*</sup>

<sup>1</sup>*Institute of Physics, Chinese Academy of Sciences, Beijing 100190, China*

<sup>2</sup>*School of Physical Sciences, University of Chinese Academy of Sciences, Beijing 100049, China*

<sup>3</sup>*Hefei National Laboratory, Hefei, 230088, China*

(Dated: January 16, 2025)

Large-scale fault-tolerant superconducting quantum computation needs rapid quantum communication to network qubits fabricated on different chips and long-range couplers to implement efficient quantum error-correction codes. Quantum channels used for these purposes are best modeled by multimode resonators, which lie between single-mode cavities and waveguides with a continuum of modes. In this Letter, we propose a formalism for quantum state transfer using coupling strengths comparable to the channel’s free spectral range ( $g \sim \Delta_{\text{fsr}}$ ). Our scheme merges features of both the STIRAP-based methods for single-mode cavities and the pitch-and-catch protocol for long waveguides, integrating their advantage of low loss and high speed. It is immune to thermal channel occupations if using harmonic resonators for the sender and receiver.

Practical quantum computation may require millions of qubits [1], while state-of-art technology holds only hundreds of qubits on a single superconducting processor [2]. Thus, it is necessary to network many processors by shuttling quantum information and distributing quantum entanglement [3] using schemes of quantum state transfer (QST), in the same manner of quantum internet [4, 5]. To connect processors kept in the same or nearby dilution fridges, we expect the quantum links to range from centimeters to a few meters. We refer to this regime as *medium range*, in order to distinguish it from the cases of extremely short or long distances. Light-matter interaction in this regime is also relevant to long-range couplers that are necessary for quantum low-density-parity-check error-correction codes to significantly save the overhead of physical qubits [6, 7]. Although QST has been extensively studied [8–30], the medium-range QST needs to be revisited, for the following reasons.

As depicted in Fig. 1, the simplest setup of QST consists of two transmon qubits [31] connected by a quantum channel. The channel supports standing waves with free spectrum range  $\Delta_{\text{fsr}}$ , which is reversely proportional to the channel length. To accurately model the system, one must compare the qubit-channel coupling strength  $g$  with  $\Delta_{\text{fsr}}$ . For *short-range* channels where  $\Delta_{\text{fsr}} \gg g$ , only the mode closest to resonance is relevant. The channel is thus modeled by a single-mode cavity and QST with high fidelity is achieved by methods based on Stimulated-Raman-Adiabatic-Passage (STIRAP) [32, 33]. For *long-range* channels where  $\Delta_{\text{fsr}} \rightarrow 0$ , the channel modes can be viewed as a continuum. In this case, Cirac, Zoller, Kimble and Mabuchi (CZKM) [8] proposed a QST protocol based on the input-output formalism and cascaded dynamics [34, 35]. It is also referred to as the *pitch-and-catch* or *relay* method [36]. The CZKM scheme has three steps (1) pitch: qubit A emits a shaped photon; (2) the photon flies to qubit B; (3) catch: B absorbs this photon through controlled interaction.

However, medium-range QST has not received suf-

ficient theoretical attention despite emerging experiments [23–30]. Transmon-waveguide couplings typically have  $g \lesssim 2\pi \times 10^2 \text{MHz}$  [37, 38]. A quick estimation shows that medium-range  $\Delta_{\text{fsr}}$  is comparable to the attainable  $g$  so that the multimode nature is essential. In this regime, the old practice of the CZKM scheme is questionable because the prerequisites of cascaded system and Markovian input-output formalism are inapplicable. The STIRAP-based methods are also suboptimal because one has to suppress  $g$  intentionally to prevent the involvement of multiple channel modes with a price of long scheme time hence the risks of qubit dissipation. Such tradeoff stimulated “hybrid” method employing STIRAP bright states to trade channel-loss-immunity for faster QST [20, 23–25]. Nevertheless, to operate QST in the regime of  $g \sim \Delta_{\text{fsr}}$ , we need to treat multiple channel modes coherently in a theory which goes beyond STIRAP and CZKM.

In this Letter, we develop a new QST formalism which

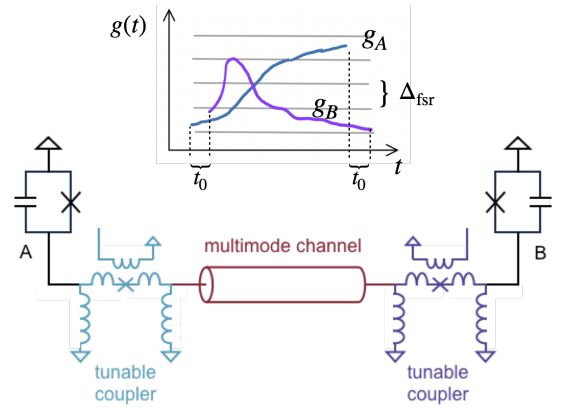


Figure 1. Schematic of the settings. Two qubits (labeled by A and B) are connected by a channel through two tunable couplers. The coupling  $g_A(t)$  and  $g_B(t)$  are activated sequentially with a delay of  $t_0 = \pi/\Delta_{\text{fsr}}$ . Our scheme enables couplings with strength comparable with  $\Delta_{\text{fsr}}$ .

reduces to STIRAP and the CZKM scheme at the short and long-range limits, respectively, consolidating their benefits of low loss and high speed from each of them. We notice that dynamics in the regime of  $g \sim \Delta_{\text{fsr}}$  is also interested in other fields [39–43].

*System and Model.* We study the settings outlined in Fig. 1, where two qubits (labeled by  $A$  and  $B$ ) are interconnected via a channel using two tunable couplers [44]. The qubits have the same transition frequency  $\omega_0$ , and the channel contains a set of equally-spaced (by  $\Delta_{\text{fsr}}$ ) discrete levels with frequency  $\{\omega_k\}_k$ . The Hamiltonian under the rotating-wave approximation reads

$$H(t) = g_A(t) \hat{\sigma}_A^\dagger \sum_k \hat{c}_k e^{-i\delta_k t} + g_B(t) \hat{\sigma}_B^\dagger \sum_k (-1)^k \hat{c}_k e^{-i\delta_k t} + \text{H.c.} \quad (1)$$

where  $\hat{\sigma}_{A/B}^\dagger$  is the qubit creation operator,  $c_k$  denotes the channel annihilation operator,  $\delta_k = \omega_k - \omega_0$ , H.c. represents Hermitian conjugate, and the phase  $(-1)^k$  in the second line reflects the distinct spatial profiles of even and odd channel modes [30, 45]. QST is described by the evolution of the state

$$|\Psi(t)\rangle = \alpha(t) |1\rangle_A + \beta(t) |1\rangle_B + \sum_k c_k(t) |1\rangle_k, \quad (2)$$

where  $\alpha(t)$ ,  $\beta(t)$  and  $c_k(t)$  are superposition coefficients and  $|1\rangle_A$ ,  $|1\rangle_B$  and  $|1\rangle_k$  denote the state with a single excitation in qubit  $A$ ,  $B$ , and mode  $k$ , respectively. The initial state has  $\alpha(t_i) = 1$  and  $\beta(t_i) = c_k(t_i) = 0$ . The target is to determine the profiles of  $g_{A/B}(t)$  to achieve  $\beta = 1$  in the end.

To start, it is observed that A couples to a collective operator  $\sum_k \hat{c}_k e^{-i\delta_k t}$  in  $H(t)$ , and the same operator couples to B in  $H(t + t_0)$  with  $t_0 = \pi/\Delta_{\text{fsr}}$ . This observation inspires us to delay  $g_B(t)$  relative to  $g_A(t)$  by  $t_0$ , cf. Fig. 1, to ensure proper response of B to A. This retardation is further justified by causality: For standard waveguides where  $\omega_k = k\Delta_{\text{fsr}}$  ( $\forall k \geq 1$ ),  $t_0$  is exactly the time a photon takes to propagate from A to B. We introduce a tilde over notations to indicate the shift of the reference of time, e.g.,  $\tilde{\beta}(t) \equiv \beta(t + t_0)$ . It is convenient to apply the convention that  $g_A(t) = \tilde{g}_B(t) = 0$  for  $t < t_i$  and  $t > t_f$ , where  $t_f$  marks the completion of the control. This convention leads to a formula for  $c_k(t_f + t_0)$ , or equivalently  $\tilde{c}_k(t_f)$  [46],

$$\tilde{c}_k(t_f) = -i \int_{t_i}^{t_f} d\tau \left[ g_A^*(\tau) \alpha(\tau) + \tilde{g}_B^*(\tau) \tilde{\beta}(\tau) \right] e^{i\delta_k \tau}, \quad (3)$$

where we have absorbed a factor of  $e^{i\omega_0 t_0}$  into the definition of  $\tilde{g}_B$ . QST is successful only if  $\tilde{c}_k(t_f) = 0$ ,  $\forall k$ . Note that Eq. (3) vanishes as long as terms in the square bracket are orthogonal to  $\exp(i\delta_k \tau) \forall k$  in the space of square-integrable functions over  $\tau \in [t_i, t_f]$ . Though not

unique, the most appealing choice for the terms in the square bracket of Eq. (3) might be simply zero,

$$g_A^*(\tau) \alpha(\tau) + \tilde{g}_B^*(\tau) \tilde{\beta}(\tau) = 0. \quad (4)$$

Equation (4) is different from the standard STIRAP dark state condition by a delay of  $t_0$  between the two terms. Thus, we refer to it as the *asynchronous dark state condition* (ADSC). A few lines of calculation shows that ADSC implies the channel mode formula [46]

$$c_k(t) = -i \int_{t-t_0}^t d\tau g_A^*(\tau) \alpha(\tau) e^{i\delta_k \tau}, \quad (5)$$

and the equations for qubit amplitudes

$$\dot{\alpha}(t) = -g_A(t) \int_{t-t_0}^t d\tau K(t-\tau) g_A^*(\tau) \alpha(\tau), \quad (6a)$$

$$\dot{\tilde{\beta}}(t) = \tilde{g}_B(t) \int_t^{t+t_0} d\tau K(t-\tau) \tilde{g}_B^*(\tau) \tilde{\beta}(\tau), \quad (6b)$$

where  $K(t-\tau) = \sum_k e^{-i\delta_k(t-\tau)}$ .

These formulae display two notable features. Firstly, Eqs. (6a) and (6b) are formally decoupled: The interplay between the two qubits disappears from the equations of motion. This is unusual because when the system is not cascaded there are often complicated feed-back or forward written in the equations of motions, see for example Refs. [47, 48]. Secondly, we learn from the integral limits of Eqs. (5) and (6) that ADSC leads to a finite memory time bounded by  $t_0$ , irrespective of the system specifications. We shall see below that these two pivotal features are the driving force behind every aspect of our scheme.

*Interpolation between STIRAP and CZKM.* Here we demonstrate that STIRAP and the CZKM scheme can be reproduced from our formalism. For STIRAP, taking the short-channel limit  $t_0 \rightarrow 0$  formally reduces Eq. (4) into the standard STIRAP dark state condition. However, the conceptual difference is that, actually,  $t_0 = 0$  is the limit of  $\Delta_{\text{fsr}} \rightarrow \infty$  where all channel modes are far blue detuned and no effective coupling occurs. In contrast, we shall see that by keeping a finite  $t_0$  explicitly, ADSC (4) can be satisfied without the adiabatic approximation, which underlies the standard STIRAP and results in slow evolutions [45, 49].

The CZKM scheme uses cascaded setups and Markovian channels where  $K(t) \propto \delta(t)$ . Here, the formal decoupling of Eqs. (6a) and (6b) is akin to cascaded dynamics. Beyond the Markovian limit, our ADSC-based formalism extends the validity of the CZKM pulses to a regime having not been envisioned. That is, if there are many discrete modes below and above the qubit frequency  $\omega_0$  and the coupling is not too strong, the kernel  $K(t)$  would be approximated by [50]

$$K(t) \propto \lim_{N \rightarrow \infty} \sum_{k=-N}^N e^{-ik\Delta_{\text{fsr}} t} \propto 2t_0 \sum_{n=-\infty}^{\infty} \delta(t-2nt_0), \quad (7)$$

Note that only the term of  $n = 0$  in the summation survives when the above formula is substituted into Eqs. (6). In this case, Eq. (6) is effectively Markovian. It explains the numerical observation that the CZKM scheme works well in some intermediate regimes [51].

*General Solutions.* Now we are in a position to find the solutions of Eq. (6) satisfying ADSC. As functions of time,  $g_A(t)$  and  $g_B(t)$  have infinitely many degrees of freedom. ADSC is a constraint that reduces these degrees of freedom by half. Thus, one strategy is to choose an arbitrary  $g_A(t)$  and then find the corresponding  $g_B(t)$ . The key factor for this strategy to work is the formal decoupling of Eq. (6a) and Eq. (6b). To proceed, for any given  $g_A(t)$ , we substitute it into Eq. (6a) and obtain the trajectory  $\alpha(t)$ . This  $g_A(t)$  is accepted as long as  $\alpha(t_f) = 0$  (up to an exponentially small correction). Suppose that such a pair of  $[g_A(t), \alpha(t)]$  is obtained. The product  $x(t) \equiv g_A^*(t)\alpha(t)$  is thus known and ADSC implies that  $\tilde{g}_B^*(t)\tilde{\beta}(t) = -x(t)$ . Next, we define the abbreviation  $y(t) \equiv -\dot{\tilde{\beta}}(t)/\tilde{g}_B(t)$  which is determined by

$$y(t) = \int_t^{t+t_0} d\tau K(t-\tau)x(\tau). \quad (8)$$

Then Eq. (6b) can be rephrased as

$$\tilde{\beta}^*(t)\dot{\tilde{\beta}}(t) = x^*(t)y(t), \quad (9)$$

The real part of Eq. (9) implies that

$$\frac{d}{dt} \left| \tilde{\beta}(t) \right|^2 = 2 \operatorname{Re} [x^*(t)y(t)], \quad (10)$$

which completely determines the magnitude of  $\tilde{\beta}(t)$ . The imaginary part of Eq. (9) implies that

$$\left| \tilde{\beta}(t) \right|^2 \frac{d}{dt} \arg \tilde{\beta}(t) = \operatorname{Im} [x^*(t)y(t)], \quad (11)$$

which fixes the phase of  $\tilde{\beta}(t)$ . Now  $\tilde{\beta}(t)$  is known and  $\tilde{g}_B(t)$  is simply  $-x^*(t)/\tilde{\beta}^*(t)$ . One can verify the ADSC results by substituting the pair of  $[g_A(t), \tilde{g}_B(t)]$  into the original Schrödinger equation.

In the end, the problem is reduced to the general existence of such  $g_A(t)$  so that Eq. (6a) produces  $\alpha(t_f) \approx 0$ . We cannot prove it rigorously but merely argue the existence using the constant ansatz  $g_A(t) = g$ . [To satisfy ADSC,  $g_A(t)$  must ramp up from zero. If the ramping is quick,  $g_A(t)$  can be approximately viewed as a constant.] We assume  $t_i = 0$  for brevity and obtain the inverse Laplace transformation of Eq. (6a)

$$\alpha(t) = \int_{\epsilon-i\infty}^{\epsilon+i\infty} \frac{e^{st} ds}{2\pi i} \left[ s + g^2 \sum_k \frac{1 - e^{-(s+i\delta_k)t_0}}{s + i\delta_k} \right]^{-1}, \quad (12)$$

where  $\epsilon > 0$ . We find that, due to the finite memory time  $t_0$  of Eq. (6a), all the poles of the integrand have negative

real parts [46]. Thus, according to Cauchy's residue theorem,  $\alpha(t)$  is a sum of exponential decays that vanishes eventually. We have verified that such exponential decay can be fast enough [46].

To compare, if only qubit A is coupled to the channel, following the step of "pitch" of the CZKM scheme, the counterpart of Eq. (6a) will include the full history of  $\alpha(t)$ . Now all the poles of its Laplace transformation locate on the imaginary axis [46] so that  $\alpha(t)$  is a sum of harmonic oscillations.

*Robustness to noises.* QST is affected by the losses from both the qubits and the channel. Denote the qubit loss rate by  $\gamma$  and the channel loss rate by  $\kappa$ . Generally we have  $\gamma < \kappa$  and the infidelity of QST is estimated by  $\gamma T + (\kappa - \gamma)\mathcal{E}$ , where  $T = t_f - t_i + t_0$  is the scheme time, and  $\mathcal{E}$  is integrated channel population [46]

$$\begin{aligned} \mathcal{E} &\equiv \sum_k \int_{t_i}^{t_f+t_0} |c_k(t)|^2 dt \\ &= t_0 + \int_{t_i}^{t_f} \tau \frac{d}{d\tau} \left[ |\alpha(\tau)|^2 + |\tilde{\beta}(\tau)|^2 \right] d\tau. \end{aligned} \quad (13)$$

To protect QST from the losses, smaller  $T$  and  $\mathcal{E}$  are favored. It is conceivable that  $T$  can be much smaller than the STIRAP-based methods because our scheme allows stronger couplings  $g \sim \Delta_{\text{fsr}}$ . As to  $\mathcal{E}$ , we find it remains small for any realizations of  $g_A(t)$  and  $g_B(t)$  as long as ADSC is obeyed [46]. Briefly, by substituting Eqs. (4) and (6) into Eq. (13), we find that the second term of Eq. (13) scales as  $O(t_*)$ , where  $t_*$  is the memory time of Eq. (6), i.e., the smaller one of  $t_0$  (imposed by ADSC) and the intrinsic memory time determined by the channel kernel  $K(t)$ . For medium-range channels, we have  $t_* = t_0$  thus  $\mathcal{E} = O(t_0)$ . It is important that here  $T$  is not relevant to  $\mathcal{E}$  so that the tradeoff between  $T$  and  $\mathcal{E}$  [20] is resolved in our QST formalism. For channels with Markovian kernel ( $t_* = 0$ ), Eq. (13) reproduces the loss of flying photon  $\mathcal{E} = t_0$ .

For realistic superconducting circuits, QST will be affected by qubit level leakage [52–56] and the dissipation from qubits and channels. The robustness of our protocol against these issues will be demonstrated numerically in the Supplemental Material [46]. Particularly, our QST scheme is also immune to thermal channel occupations if using harmonic oscillators as the sender and receiver, same with Refs. [16, 17] but in a broader regime.

*Examples.* As a demonstration of principle, we accommodate ourselves by considering two scenarios where the kernel  $K(t)$ , control pulses  $g_{A/B}(t)$  and amplitudes  $\alpha(\beta)$  are all real-valued. In Case 1,  $\omega_0$  is in the middle of two channel modes (detuned by  $\pm\Delta_{\text{fsr}}/2$ ), see the inset of Fig. 2(a). In Case 2,  $\omega_0$  is resonant with one channel mode, see the inset of Fig. 3(a). Each case involves an equal number of channel modes above and below  $\omega_0$ , set here to be three. We unintentionally choose  $g_A(t) = g + g \sin[(t-5)/(10\pi)]$ , where  $g/\Delta_{\text{fsr}} = 0.15 \sim 0.4$

(in increments of 0.05, distinguished by colors) and  $t$  denotes time in units of  $2\pi/\Delta_{\text{fsr}}$  (thus  $t_0 = 0.5$ ). Our computations utilize the Python IDEsolver package [57] to solve Eq. (6a) and determine  $\tilde{g}_B(t)$ . We then validate the control pulses by solving the original Schrödinger equation using QuTiP [58, 59], and compare the results of  $\alpha(t)$  and  $\tilde{\beta}(t)$  with the predictions of ADSC-based formulae. Numerical results for these two scenarios are shown in Figs. 2 and 3, respectively.

In Fig. 2(a) we plot the shapes of  $g_A(t)$  (dashed curves) and the companion  $\tilde{g}_B(t)$  (solid curves) obtained by the method introduced above. We then substitute the control pulses into the original Schrödinger equation and obtain the results of  $1 - |\alpha(t)|^2$  and  $1 - |\tilde{\beta}(t)|^2$  depicted in Fig. 2(b). The curves confirm that stronger  $g_A$  facilitates faster QST. The results shown in Fig. 2(b) are compared with results calculated by Eqs. (6a) and (10). Their discrepancies are found to be smaller than  $10^{-6}$ , as plotted in Fig. 2(c). This error is further reduced by decreasing the temporal step length (set at  $\Delta t = 0.002$ ) in the numerical calculations. To assess the risk of channel loss, we plot the channel population  $\sum_k |c_k(t)|^2$  in Fig. 2(d), accompanied by the integrated population  $\mathcal{E}$  (13) for each  $g/\Delta_{\text{fsr}}$ . The results corroborate our analysis that  $\mathcal{E} = O(t_0)$ , and, somewhat surprisingly,  $\mathcal{E}$  is almost in-

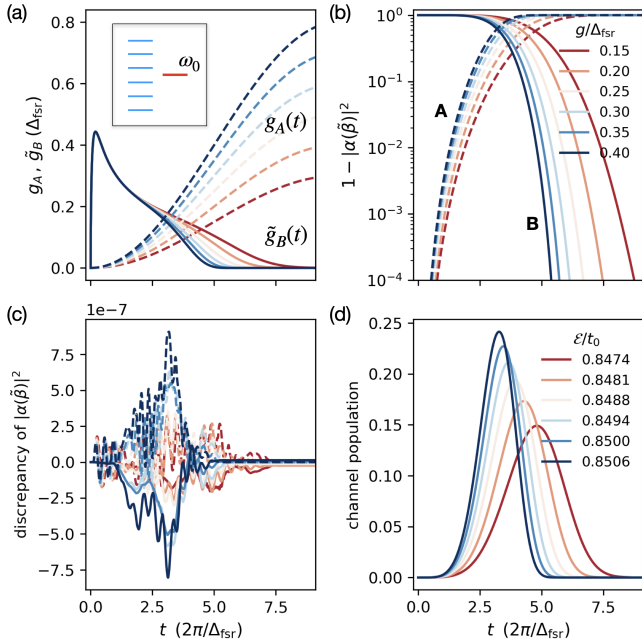


Figure 2. Numerical results for the setup with level structure depicted in the inset of (a), which contains six channel modes. (a)  $g_A$  (dashed curves) and the companion  $\tilde{g}_B$  (solid). (b) Reversed populations  $1 - |\alpha|^2$  (dashed curves) and  $1 - |\tilde{\beta}|^2$  (solid curves) calculated from the original Schrödinger equation. (c) The discrepancies between the original Schrödinger equation and the ADSC-based equations: Dashed curves for  $|\alpha|^2$ , and solid curves for  $|\tilde{\beta}|^2$ . (d) Channel populations and the table of the integrated population  $\mathcal{E}/t_0$ .

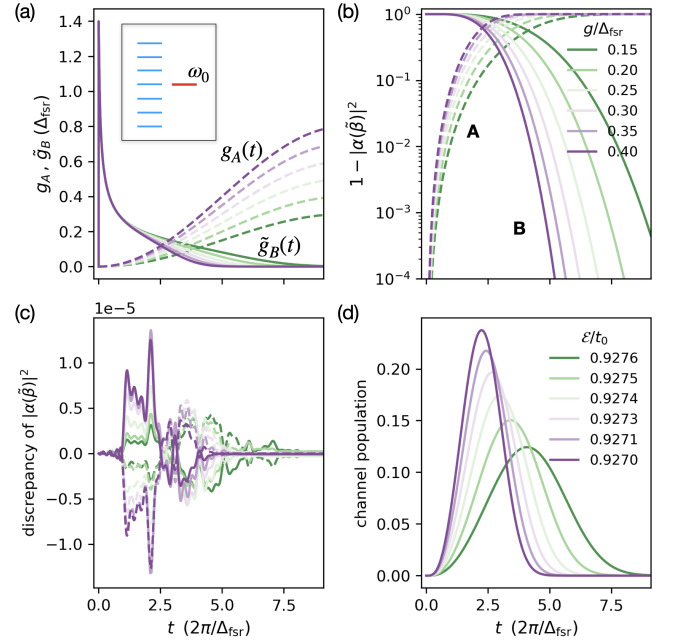


Figure 3. Numerical results for the setup with level structures depicted in the inset of (a), which contains seven channel modes. The subplots (a-d) are arranged in the same manner of Fig. 2.

variant with respect to  $g/\Delta_{\text{fsr}}$ .

Figure 3 conveys the similar message. Notably, the control sequences  $\tilde{g}_B(t)$  shown in Fig. 3(a) exhibit higher peaks. The discrepancies between the full Schrödinger equation and ADSC predictions are at the level of  $10^{-5}$  (obtained with  $\Delta t = 0.001$ ), cf. Fig. 3(c). The integrated channel population is 0.927 for all values of  $g/\Delta_{\text{fsr}}$ , exceeding that observed in Fig. 2(d) by approximately 10%. This may elucidate the estimation that the level configuration of Case 2 yields higher fidelity [60].

*Conclusion.* In this Letter, we have developed a formalism for QST through a multimode channel. This central idea is to control the system time-dependently to satisfy ADSC (4). Our approach integrates key features of both STIRAP and the CZKM scheme, enabling QST implementation with coupling strengths comparable to the free spectral range of the channel  $g \sim \Delta_{\text{fsr}}$ . The increased coupling strengths give rise to faster QST, which is favored for minimizing qubit loss. Meanwhile, the risk of channel loss scales as  $O(\kappa t_0)$ , where  $t_0 = \pi/\Delta_{\text{fsr}}$ , independent of system specifications. The level of loss is acceptable because  $t_0$  is typically much smaller than the QST scheme time. Our results have potential applications in the realization of fast and reliable chip-to-chip quantum communication, entanglement distribution, and couplers between non-neighboring qubits, which are crucial for large scale fault-tolerant quantum computation. For future works, one may propose other strategies for solving Eq. (6) and optimize the control pulses under re-

alistic conditions. Remote quantum logic gates and frequency/time division multiplexing based on ADSC (4) might also be interesting topics.

Y.-X. Z. thanks the discussions with Y. Zhong and the comments from J. J. García-Rippoll, and acknowledges the financial support from Innovation Program for Quantum Science and Technology (Grant No. 2023ZD0301100 and No. 2-6), National Natural Science Foundation of China (Grant No. 12375024), and CAS Project for Young Scientists in Basic Research (YSBR-100).

---

\* [iyxz@iphy.ac.cn](mailto:iyxz@iphy.ac.cn)

- [1] A. G. Fowler, M. Mariantoni, J. M. Martinis, and A. N. Cleland, *Phys. Rev. A* **86**, 032324 (2012).
- [2] D. Castelvecchi, *Nature* **624**, 238 (2023).
- [3] S. Bravyi, O. Dial, J. M. Gambetta, D. Gil, and Z. Nazario, *Journal of Applied Physics* **132** (2022), 10.1063/5.0082975.
- [4] H. J. Kimble, *Nature* **453**, 1023 (2008).
- [5] S. Wehner, D. Elkouss, and R. Hanson, *Science* **362**, eaam9288 (2018).
- [6] N. Baspin and A. Krishna, *Quantum* **6**, 711 (2022).
- [7] S. Bravyi, A. W. Cross, J. M. Gambetta, D. Maslov, P. Rall, and T. J. Yoder, *Nature* **627**, 778 (2024).
- [8] J. I. Cirac, P. Zoller, H. J. Kimble, and H. Mabuchi, *Phys. Rev. Lett.* **78**, 3221 (1997).
- [9] M. Christandl, N. Datta, A. Ekert, and A. J. Landahl, *Phys. Rev. Lett.* **92**, 187902 (2004).
- [10] W. Yao, R.-B. Liu, and L. J. Sham, *Phys. Rev. Lett.* **95**, 030504 (2005).
- [11] A. Kay, *International Journal of Quantum Information* **08**, 641 (2010).
- [12] A. N. Korotkov, *Phys. Rev. B* **84**, 014510 (2011).
- [13] L. Steffen, Y. Salathe, M. Oppliger, P. Kurpiers, M. Baur, C. Lang, C. Eichler, G. Puebla-Hellmann, A. Fedorov, and A. Wallraff, *Nature* **500**, 319 (2013).
- [14] J. Wenner, Y. Yin, Y. Chen, R. Barends, B. Chiaro, E. Jeffrey, J. Kelly, A. Megrant, J. Y. Mutus, C. Neill, P. J. J. O'Malley, P. Roushan, D. Sank, A. Vainsencher, T. C. White, A. N. Korotkov, A. N. Cleland, and J. M. Martinis, *Phys. Rev. Lett.* **112**, 210501 (2014).
- [15] A. Reiserer and G. Rempe, *Rev. Mod. Phys.* **87**, 1379 (2015).
- [16] Z.-L. Xiang, M. Zhang, L. Jiang, and P. Rabl, *Phys. Rev. X* **7**, 011035 (2017).
- [17] B. Vermersch, P.-O. Guimond, H. Pichler, and P. Zoller, *Phys. Rev. Lett.* **118**, 133601 (2017).
- [18] C. J. Axline, L. D. Burkhardt, W. Pfaff, M. Zhang, K. Chou, P. Campagne-Ibarcq, P. Reinhold, L. Frunzio, S. M. Girvin, L. Jiang, M. H. Devoret, and R. J. Schoelkopf, *Nature Physics* **14**, 705 (2018).
- [19] P. Kurpiers, P. Magnard, T. Walter, B. Royer, M. Pechal, J. Heinsoo, Y. Salathé, A. Akin, S. Storz, J. C. Besse, S. Gasparinetti, A. Blais, and A. Wallraff, *Nature* **558**, 264 (2018).
- [20] Y.-D. Wang and A. A. Clerk, *New Journal of Physics* **14**, 105010 (2012).
- [21] P. Magnard, S. Storz, P. Kurpiers, J. Schär, F. Marxer, J. Lütolf, T. Walter, J.-C. Besse, M. Gabureac, K. Reuer, A. Akin, B. Royer, A. Blais, and A. Wallraff, *Phys. Rev. Lett.* **125**, 260502 (2020).
- [22] L. D. Burkhardt, J. D. Teoh, Y. Zhang, C. J. Axline, L. Frunzio, M. H. Devoret, L. Jiang, S. M. Girvin, and R. J. Schoelkopf, *PRX Quantum* **2**, 030321 (2021).
- [23] A. Bienfait, K. J. Satzinger, Y. P. Zhong, H.-S. Chang, M.-H. Chou, C. R. Conner, É. Dumur, J. Grebel, G. A. Peairs, R. G. Povey, and A. N. Cleland, *Science* **364**, 368 (2019).
- [24] Y. Zhong, H.-S. Chang, A. Bienfait, É. Dumur, M.-H. Chou, C. R. Conner, J. Grebel, R. G. Povey, H. Yan, D. I. Schuster, and A. N. Cleland, *Nature* **590**, 571 (2021).
- [25] J. Niu, L. Zhang, Y. Liu, J. Qiu, W. Huang, J. Huang, H. Jia, J. Liu, Z. Tao, W. Wei, Y. Zhou, W. Zou, Y. Chen, X. Deng, X. Deng, C. Hu, L. Hu, J. Li, D. Tan, Y. Xu, F. Yan, T. Yan, S. Liu, Y. Zhong, A. N. Cleland, and D. Yu, *Nature Electronics* **6**, 235 (2023).
- [26] J. Grebel, H. Yan, M.-H. Chou, G. Andersson, C. R. Conner, Y. J. Joshi, J. M. Miller, R. G. Povey, H. Qiao, X. Wu, and A. N. Cleland, *Phys. Rev. Lett.* **132**, 047001 (2024).
- [27] D. C. McKay, R. Naik, P. Reinhold, L. S. Bishop, and D. I. Schuster, *Phys. Rev. Lett.* **114**, 080501 (2015).
- [28] N. M. Sundaesan, Y. Liu, D. Sadri, L. J. Szócs, D. L. Underwood, M. Malekakhlagh, H. E. Türeci, and A. A. Houck, *Phys. Rev. X* **5**, 021035 (2015).
- [29] S. Chakram, K. He, A. V. Dixit, A. E. Oriani, R. K. Naik, N. Leung, H. Kwon, W.-L. Ma, L. Jiang, and D. I. Schuster, *Nature Physics* **18**, 879 (2022).
- [30] H.-S. Chang, Y. P. Zhong, A. Bienfait, M.-H. Chou, C. R. Conner, E. Dumur, J. Grebel, G. A. Peairs, R. G. Povey, K. J. Satzinger, and A. N. Cleland, *Phys. Rev. Lett.* **124**, 240502 (2020).
- [31] J. Koch, T. M. Yu, J. Gambetta, A. A. Houck, D. I. Schuster, J. Majer, A. Blais, M. H. Devoret, S. M. Girvin, and R. J. Schoelkopf, *Phys. Rev. A* **76**, 042319 (2007).
- [32] N. V. Vitanov, A. A. Rangelov, B. W. Shore, and K. Bergmann, *Rev. Mod. Phys.* **89**, 015006 (2017).
- [33] K. Bergmann, H.-C. Nägerl, C. Panda, G. Gabrielse, E. Miloglyadov, M. Quack, G. Seyfang, G. Wichmann, S. Ospelkaus, A. Kuhn, S. Longhi, A. Szameit, P. Pirro, B. Hillebrands, X.-F. Zhu, J. Zhu, M. Drewsen, W. K. Hensinger, S. Weidt, T. Halfmann, H.-L. Wang, G. S. Paraoanu, N. V. Vitanov, J. Mompart, T. Busch, T. J. Barnum, D. D. Grimes, R. W. Field, M. G. Raizen, E. Narevicius, M. Auzinsh, D. Budker, A. Pálffy, and C. H. Keitel, *Journal of Physics B: Atomic, Molecular and Optical Physics* **52**, 202001 (2019).
- [34] C. W. Gardiner, *Phys. Rev. Lett.* **70**, 2269 (1993).
- [35] H. J. Carmichael, *Phys. Rev. Lett.* **70**, 2273 (1993).
- [36] Y. Zhong, H.-S. Chang, K. Satzinger, M.-H. Chou, A. Bienfait, C. Conner, É. Dumur, J. Grebel, G. Peairs, R. Povey, *et al.*, *Nature Physics* **15**, 741 (2019).
- [37] M. Mirhosseini, E. Kim, X. Zhang, A. Sipahigil, P. B. Dieterle, A. J. Keller, A. Asenjo-Garcia, D. E. Chang, and O. Painter, *Nature* **569**, 692 (2019).
- [38] A. S. Sheremet, M. I. Petrov, I. V. Iorsh, A. V. Poshakinskiy, and A. N. Poddubny, *Rev. Mod. Phys.* **95**, 015002 (2023).
- [39] D. O. Krimer, M. Liertzner, S. Rotter, and H. E. Türeci, *Phys. Rev. A* **89**, 033820 (2014).
- [40] X. Han, C.-L. Zou, and H. X. Tang, *Phys. Rev. Lett.* **117**, 123603 (2016).

- [41] A. Johnson, M. Blaha, A. E. Ulanov, A. Rauschenbeutel, P. Schneeweiss, and J. Volz, *Phys. Rev. Lett.* **123**, 243602 (2019).
- [42] D. Lechner, R. Pernetta, M. Blaha, P. Schneeweiss, A. Rauschenbeutel, and J. Volz, *Phys. Rev. Lett.* **131**, 103603 (2023).
- [43] D. Lentrodt, O. Diekmann, C. H. Keitel, S. Rotter, and J. Evers, *Phys. Rev. Lett.* **130**, 263602 (2023).
- [44] Y. Chen, C. Neill, P. Roushan, N. Leung, M. Fang, R. Barends, J. Kelly, B. Campbell, Z. Chen, B. Chiaro, A. Dunsworth, E. Jeffrey, A. Megrant, J. Y. Mutus, P. J. J. O’Malley, C. M. Quintana, D. Sank, A. Vainsencher, J. Wenner, T. C. White, M. R. Geller, A. N. Cleland, and J. M. Martinis, *Phys. Rev. Lett.* **113**, 220502 (2014).
- [45] M. Malekakhlagh, T. Phung, D. Puzzuoli, K. Heya, N. Sundaresan, and J. Orcutt, “Enhanced quantum state transfer and bell state generation over long-range multimode interconnects via superadiabatic transitionless driving,” (2024), [arXiv:2401.09663 \[quant-ph\]](https://arxiv.org/abs/2401.09663).
- [46] *Supplemental Material contains detailed derivations and the numerical evidence for the robustness to various noises. It includes Refs. [61, 62].*
- [47] K. Sinha, A. González-Tudela, Y. Lu, and P. Solano, *Phys. Rev. A* **102**, 043718 (2020).
- [48] Y.-X. Zhang, *Phys. Rev. Lett.* **131**, 193603 (2023).
- [49] A. Baksic, H. Ribeiro, and A. A. Clerk, *Phys. Rev. Lett.* **116**, 230503 (2016).
- [50] P. W. Milonni, J. R. Ackerhalt, H. W. Galbraith, and M.-L. Shih, *Phys. Rev. A* **28**, 32 (1983).
- [51] G. F. Peñas, R. Puebla, T. Ramos, P. Rabl, and J. J. García-Ripoll, *Phys. Rev. Appl.* **17**, 054038 (2022).
- [52] D. Sank, Z. Chen, M. Khezri, J. Kelly, R. Barends, B. Campbell, Y. Chen, B. Chiaro, A. Dunsworth, A. Fowler, E. Jeffrey, E. Lucero, A. Megrant, J. Mutus, M. Neeley, C. Neill, P. J. J. O’Malley, C. Quintana, P. Roushan, A. Vainsencher, T. White, J. Wenner, A. N. Korotkov, and J. M. Martinis, *Phys. Rev. Lett.* **117**, 190503 (2016).
- [53] F. Battistel, B. Varbanov, and B. Terhal, *PRX Quantum* **2**, 030314 (2021).
- [54] B. M. Varbanov, F. Battistel, B. M. Tarasinski, V. P. Ostroukh, T. E. O’Brien, L. DiCarlo, and B. M. Terhal, *npj Quantum Information* **6**, 102 (2020).
- [55] N. Lacroix, L. Hafele, A. Remm, O. Benhayoune-Khadraoui, A. McDonald, R. Shillito, S. Lazar, C. Hellings, F. Swiadek, D. Colao-Zanuz, A. Flasby, M. B. Panah, M. Kerschbaum, G. J. Norris, A. Blais, A. Wallraff, and S. Krinner, “Fast flux-activated leakage reduction for superconducting quantum circuits,” (2023), [arXiv:2309.07060 \[quant-ph\]](https://arxiv.org/abs/2309.07060).
- [56] M. McEwen, D. Kafri, Z. Chen, J. Atalaya, K. J. Satzinger, C. Quintana, P. V. Klimov, D. Sank, C. Gidney, A. G. Fowler, F. Arute, K. Arya, B. Buckley, B. Burkett, N. Bushnell, B. Chiaro, R. Collins, S. Demura, A. Dunsworth, C. Erickson, B. Foxen, M. Giustina, T. Huang, S. Hong, E. Jeffrey, S. Kim, K. Kechedzhi, F. Kostritsa, P. Laptev, A. Megrant, X. Mi, J. Mutus, O. Naaman, M. Neeley, C. Neill, M. Niu, A. Paler, N. Redd, P. Roushan, T. C. White, J. Yao, P. Yeh, A. Zalcman, Y. Chen, V. N. Smelyanskiy, J. M. Martinis, H. Neven, J. Kelly, A. N. Korotkov, A. G. Petukhov, and R. Barends, *Nature Communications* **12**, 1761 (2021).
- [57] J. T. Karpel, *Journal of Open Source Software* **3**, 542 (2018).
- [58] J. Johansson, P. Nation, and F. Nori, *Computer Physics Communications* **183**, 1760 (2012).
- [59] J. Johansson, P. Nation, and F. Nori, *Computer Physics Communications* **184**, 1234 (2013).
- [60] J. D. Teoh, *Error Detection in Bosonic Circuit Quantum Electrodynamics Error Detection in Bosonic Circuit Quantum Electrodynamics Error Detection in Bosonic Circuit Quantum Electrodynamics*, Ph.D. thesis, Yale University (2023).
- [61] Z. Li, P. Liu, P. Zhao, Z. Mi, H. Xu, X. Liang, T. Su, W. Sun, G. Xue, J.-N. Zhang, W. Liu, Y. Jin, and H. Yu, *npj Quantum Information* **9**, 111 (2023).
- [62] A. Marquet, S. Dupouy, U. Réglade, A. Essig, J. Cohen, E. Albertinale, A. Bienfait, T. Peronnin, S. Jezouin, R. Lescanne, and B. Huard, *Phys. Rev. Appl.* **22**, 034053 (2024).

# Supplemental Material to “Quantum State Transfer via a Multimode Resonator”

Yang He<sup>1,2</sup> and Yu-Xiang Zhang<sup>1,2,3</sup>

<sup>1</sup>*Institute of Physics, Chinese Academy of Sciences, Beijing 100190, China*

<sup>2</sup>*School of Physical Sciences, University of Chinese Academy of Sciences, Beijing 100049, China*

<sup>3</sup>*Hefei National Laboratory, Hefei, 230088, China*

(Dated: January 16, 2025)

The Supplemental Material is arranged as follows. In Sec. **I** we derive Eqs. (5,6) of the main text. In Sec. **II** we discuss the Laplace transformation of the integro-differential equation (6a) of the main text given a constant  $g_A(t) = g$ . In Sec. **III** we present the details for the claim of  $\mathcal{E} = O(t_0)$ . In Sec. **IV** we numerically study the adverse effects of qubit leakage error and qubit/channel losses. In Sec. **V** we study the robustness to thermal channel photon population.

## I. SCHRÖDINGER EQUATIONS AND ADSC

Here we derive the equations of motion using the Hamiltonian and single-excitation ansatz introduced in the main text. Schrödinger equation for the channel mode amplitude  $c_k$  reads

$$\dot{c}_k(t) = -i\alpha(t)g_A^*(t)e^{i\delta_k t} - i\beta(t)(-1)^k g_B^*(t)e^{i\delta_k t}. \quad (1)$$

Using the initial condition  $c_k(t_i) = 0$ , the above equation is formally solved by

$$c_k(t) = -i \int_{t_i}^t d\tau [g_A^*(\tau)\alpha(\tau) + (-1)^k g_B^*(\tau)\beta(\tau)] e^{i\delta_k \tau}. \quad (2)$$

Now let us replace  $g_B^*(\tau)\beta(\tau)$  by  $\tilde{g}_B^*(\tau - t_0)\tilde{\beta}(\tau - t_0)$  so that the second part is rewritten as

$$(-1)^k \int_{t_i - t_0}^{t - t_0} d\tau \tilde{g}_B^*(\tau)\tilde{\beta}(\tau) e^{i\delta_k(\tau + t_0)} \quad (3)$$

Recall the convention that  $\tilde{g}_B(t) = 0$  for  $t < t_i$  and

$$e^{i\delta_k t_0} = (-1)^k e^{-i\omega_0 t_0}. \quad (4)$$

We can also choose  $e^{i\delta_k t_0} = (-1)^{k+1} e^{-i\omega_0 t_0}$  on the right hand side of the above formula, because  $k$  is just a numbering of the channel modes. Equation (2) is then

$$c_k(t) = -i \int_{t_i}^t d\tau g_A^*(\tau)\alpha(\tau) e^{i\delta_k \tau} - i e^{-i\omega_0 t_0} \int_{t_i}^{t - t_0} d\tau \tilde{g}_B^*(\tau)\tilde{\beta}(\tau) e^{i\delta_k \tau}. \quad (5)$$

To obtain Eq. (3) of the main text, one just needs to substitute  $t = t_f + t_0$  into the above formula and use the convention that  $g_A(t) = 0$  for  $t > t_f$ , and redefine  $\tilde{g}_B(t)$  by  $e^{i\omega_0 t_0} \tilde{g}_B(t)$ .

Equations for the amplitudes of the two qubits are

$$\dot{\alpha}(t) = -ig_A(t) \sum_k e^{-i\delta_k t} c_k(t) \quad (6a)$$

$$\dot{\beta}(t) = -ig_B(t) \sum_k (-1)^k e^{-i\delta_k t} c_k(t) \quad (6b)$$

For qubit A, we substitute Eq. (5) into the above formula and obtain

$$\begin{aligned} \dot{\alpha}(t) = & -g_A(t) \int_{t_i}^t d\tau K(t - \tau) g_A^*(\tau) \alpha(\tau) \\ & - g_A(t) \int_{t_i}^{t - t_0} d\tau K(t - \tau) \tilde{g}_B^*(\tau) \tilde{\beta}(\tau) e^{-i\omega_0 t_0} \end{aligned} \quad (7)$$

Then ADSC cancels the integral over  $[t_i, t - t_0]$  hence results in Eq. (6a) of the main text. The case of qubit B is similar.

## II. DISTRIBUTION OF THE POLES

The poles of Eq. (12) of the main text are determined by solving the following equation

$$s + g^2 \sum_k \frac{1 - e^{-(s+i\delta_k)t_0}}{s + i\delta_k} = 0. \quad (8)$$

We change the variable as  $s \rightarrow i(z + \omega_0)$  and obtain

$$z + \omega_0 - g^2 \sum_k \frac{1 - (-1)^k e^{izt_0}}{z + k\Delta_{\text{fsr}}} = 0. \quad (9)$$

If there is a real solution of  $z$ , the imaginary and real parts of the above formula both vanish,

$$\sin(zt_0) \sum_k \frac{(-1)^k}{z + k\Delta_{\text{fsr}}} = 0 \quad (10a)$$

$$z + \omega_0 - g^2 \sum_k \frac{1 - (-1)^k \cos(zt_0)}{z + k\Delta_{\text{fsr}}} = 0. \quad (10b)$$

Equation (10a) implies that either  $\sin(zt_0) = 0$  or the summation vanishes. Nevertheless, it vanishes only for a countable set of values of  $z$ , which are independent to  $\omega_0$ . However,  $\omega_0$  appears in Eq. (10b) so that Eqs. (10a) and (10b) are both fulfilled only if  $\omega_0$  equals some certain values. Thus, in general there are no real solutions to  $z$ , equivalently, no purely imaginary poles of the Laplace

transformation, which means that QST will succeed up to an exponentially decreasing error.

To have an idea of how fast the exponential decay could be, we plot the slowest decay rate (largest real part of the poles  $s$ , which are negative) for the two examples studied in the main text in Fig. 1. The plot shows that QST can be efficiently implemented provided that the coupling strength  $g$  is not too small.

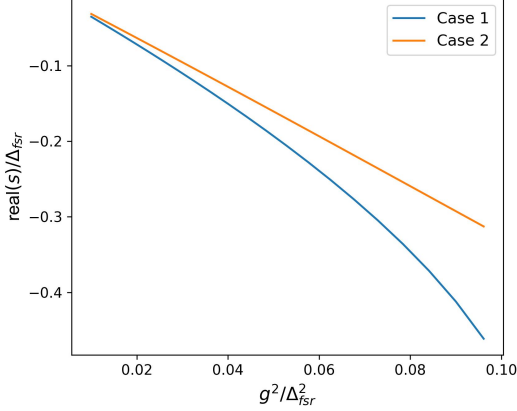


Figure 1. The largest real part of the poles (in the unit of  $\Delta_{\text{fsr}}$ ) of the Laplace transformation formula of the two cases introduced in the main text.

The above result can be compared with the integro-differential equation where the full history is included, which is exactly the equation describing the interaction between a single qubit and the channel reads

$$\dot{\alpha}(t) = -g^2 \int_0^t d\tau K(t-\tau)\alpha(\tau). \quad (11)$$

Provided that  $\alpha(0) = 1$ ,  $\alpha(t)$  is solved by

$$\alpha(t) = \int_{\sigma-i\infty}^{\sigma+i\infty} \frac{e^{st} ds}{2\pi i} \left[ s + g^2 \sum_k \frac{1}{s + i\delta_k} \right]^{-1}. \quad (12)$$

To find the poles, we change the variable as  $s \rightarrow iz$  and obtain

$$z - g^2 \sum_k \frac{1}{z + \delta_k} = 0. \quad (13)$$

As an equation with real coefficients, if  $z$  is a solution, so is  $z^*$ . One of the corresponding  $s$  of this conjugate pairs will have a positive real part. This is impossible because the Laplace transformation of a bounded function is analytic on the right half of the complex plane. Therefore, all the poles of Eq. (12) are distributed on the imaginary axis.

### III. CHANNEL LOSS

Here we derive the formula of channel loss. The normalization of state (2) of the main text simply implies

that

$$\begin{aligned} \mathcal{E} &= \int_{t_i}^{t_f+t_0} dt \sum_k |c_k(t)|^2 \\ &= t_f - t_i + t_0 - \int_{t_i}^{t_f+t_0} d\tau [|\alpha(\tau)|^2 + |\beta(\tau)|^2] \\ &= \int_{t_i}^{t_f+t_0} d\tau \tau \frac{d}{d\tau} [|\alpha(\tau)|^2 + |\beta(\tau)|^2], \end{aligned} \quad (14)$$

where we have used the formula of integration by parts in the third line. Next, the conventions that  $g_A(t > t_f) = 0$  means that

$$\int_{t_i}^{t_f+t_0} d\tau \tau \frac{d}{d\tau} |\alpha(\tau)|^2 = \int_{t_i}^{t_f} d\tau \tau \frac{d}{d\tau} |\alpha(\tau)|^2. \quad (15)$$

Similarly, we can replace  $\beta(t)$  by  $\tilde{\beta}(t)$  and the convention that  $\tilde{g}_B(t < t_i) = 0$  implies that

$$\int_{t_i}^{t_f+t_0} d\tau \tau \frac{d}{d\tau} |\beta(\tau)|^2 = t_0 + \int_{t_i}^{t_f} d\tau \tau \frac{d}{d\tau} |\tilde{\beta}(\tau)|^2. \quad (16)$$

In the end, we obtain

$$\mathcal{E} = t_0 + \int_{t_i}^{t_f} dt t \frac{d}{dt} [|\alpha(t)|^2 + |\tilde{\beta}(t)|^2]. \quad (17)$$

We refer to the unraveled integral as “(buffer)” because it vanishes if the emission from qubit A and the absorption of qubit B have the same pace.

Applying the Schrödinger equation, ADSC, and the conventions that  $g_A(t < t_i) = 0$  and  $\tilde{g}_B(t > t_f) = 0$ , we can expand the (buffer) term into

$$\begin{aligned} (\text{buffer}) &= \int_{-\infty}^{\infty} dt \int_{t-t_0}^t d\tau (t-\tau) \alpha^*(t) g_A(t) \\ &\quad \times K(t-\tau) \alpha(\tau) g_A^*(\tau) + \text{c.c.}, \end{aligned} \quad (18)$$

where “c.c.” is a shorthand of complex conjugate. Therein, let us assume When  $t_0$  is much shorter than the scheme time  $t_f - t_i$ , we can view  $t_0$  as a coarse grained scale of time within which  $g_A(t)$  and  $\alpha(t)$  change little. Then, we simply replace the factor  $(t-\tau)$  in the first line of the above formula with  $t_0$ . This is fine because  $0 \leq t-\tau \leq t_0$  by definition. It leads to

$$\begin{aligned} (\text{buffer}) &\sim t_0 \int_{-\infty}^{\infty} dt \int_{t-t_0}^t d\tau K(t-\tau) \\ &\quad \times \alpha^*(t) g_A(t) \alpha(\tau) g_A^*(\tau) + \text{c.c.} \\ &= -t_0 \int_{-\infty}^{\infty} dt \frac{d}{dt} |\alpha(t)|^2 \\ &= t_0. \end{aligned} \quad (19)$$

Therefore, the channel loss  $\kappa P$ , cf. Eq. (17), is bounded by the scale  $O(\kappa t_0)$ .

As a remark, in order to extend the above argument to long channels, one should keep in mind that the effective memory time  $t_*$  of the system is

$$t_* = \min\{t_0, t_{\text{channel}}\}, \quad (20)$$

where  $t_{\text{channel}}$  is the intrinsic memory time determined by the kernel function  $K(t \gg t_{\text{channel}}) \rightarrow 0$ . Generally speaking, we have  $t_* = t_{\text{channel}}$  for long channels, especially when the Markovian approximation works well. Thus, we should replace  $t_0$  by  $t_*$  in the estimation of the (buffer) term thereof.

#### IV. THE ROBUSTNESS TO QUBIT LEAKAGE AND QUBIT/CHANNEL LOSS

In this section, we study how the extra excitation in the sender initialization and the qubit and channel dissipation affect the efficiency of our QST scheme. The figure of merit used to characterize the influence is the inefficiency defined by

$$1 - \left| \tilde{\beta}(t_f) \right|^2, \quad (21)$$

where that  $\tilde{\beta}$  denotes the amplitude of having only a single excitation at B. Inefficiency defined above can also be understood as a measure of QST infidelity.

##### A. Qubit Leakage to Higher Levels

To account for the leakage to higher transmon levels, we set the transmon anharmonicity at  $2.5 \Delta_{\text{fsr}}$  and write the initial state of qubit A as

$$(1 - \text{er})^{0.5} |1\rangle_A + \text{er}^{0.5} |2\rangle_A,$$

where “er” quantifies the leakage error in sender’s initial state preparation. Here a coherent leakage is assumed so that qubit A is initialized in a pure state. Channel and qubit B are assumed to be in their ground states. We continue to use the controls  $g_A(t)$  and  $g_B(t)$  obtained for the ideal systems.

We solve the system evolution using QuTiP and plot QST inefficiency as a function of er in Fig. 2(a). It shows a linear relation between them, indicating the applicability of first order perturbation. Since single qubit gates with an average gate error below  $10^{-4}$  has been realized in Ref. [1], we believe that qubit leakage should not be problematic in our scheme.

To see the location of the population leakage, we plot the final population on  $|2_B\rangle$  (normalized by the factor er) in Fig. 2(b). The results show that the initial leakage at the sender will result in comparable amount of leakage into the second excited state of qubit B (the receiver). Also, we plot the total population on doubly-excited qubit states (normalized by the factor er) in Fig. 2(c).

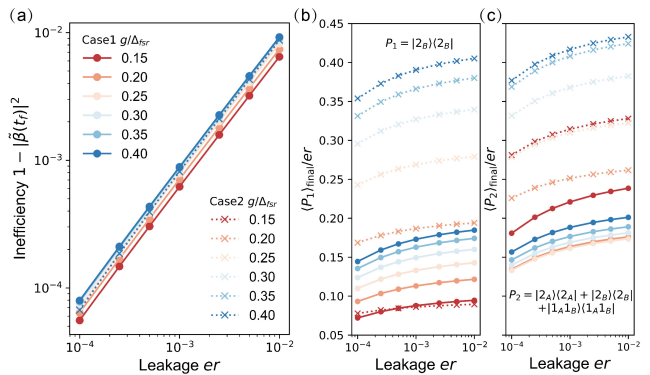


Figure 2. QST inefficiency due to qubit leakage error. (a) Inefficiency of QST,  $1 - \left| \tilde{\beta}(t_f) \right|^2$ , as the function of initial amount of leakage into  $|2_A\rangle$ , for the two examples introduced in the main text. The solid curves represent Case 1 where the qubit frequency lies in the middle of two channel modes. The dashed ones represent Case 2 where the qubits are in resonance with one channel mode. (b) The population (relative to the initial leakage er) of  $|2_B\rangle$  at the end of QST. (c) The final population (relative to the initial leakage er) on  $|2_A\rangle$ ,  $|2_B\rangle$  and  $|1_A\rangle \otimes |1_B\rangle$ .

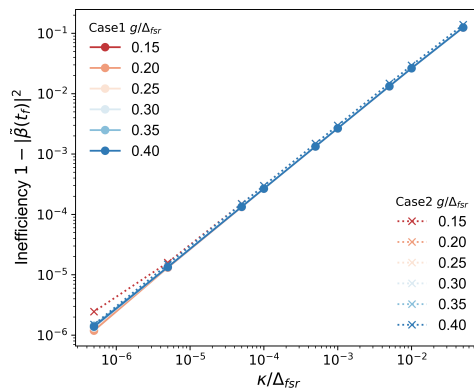


Figure 3. Transfer inefficiency due to channel decoherence  $\kappa$ .

By comparing (b) and (c) we find that using stronger couplings (blue curves) leads to less relative populations on qubit A (the sender). The population of photons left in the channel modes can be obtained from the results of qubit populations by the normalization condition. We find that it is comparable to the leakage of the qubits.

##### B. Channel Loss

When only the channel decoherence, with a rate  $\kappa$ , is considered, the inefficiency is found insensitive to the coupling strength as shown in Fig. 3. This feature reflects our analytical result that the integrated channel mode population  $\mathcal{E}$  is almost invariant with respect to  $g/\Delta_{\text{fsr}}$ .

### C. Qubit Loss

Now we assume the channel is perfect and consider the influence of qubit loss. In this case, we have to assign a terminal point of the QST scheme. This is because when there considerable populations on qubit B, it become more vulnerable to qubit decay. Thus, there must be a critical point where the highest fidelity is reached. We confirm this intuition by Fig. 4(a), which shows that the QST inefficiency goes up after reaching some minimal inefficiency, due to the exponential decay of B [to compare, the dotted curves in Fig. 4(a) show the results without qubit decay]. Therefore, we consider the transfer procedure accomplished when the inefficiency reaches its minimum, and plot the corresponding value in Fig 4(b). Without a surprise, larger  $g$  results in a faster QST and therefore less qubit loss.

In our plots, we use the free spectral range  $\Delta_{\text{fsr}}$  as the unit of frequency. If we assume that  $\Delta_{\text{fsr}} = 2\pi \times 100\text{MHz}$ , the decay rate of  $0.001\Delta_{\text{fsr}}$  corresponds to a short qubit  $T_1 \approx 1.6\mu\text{s}$ . Figures 3 and 4 shows that even under such circumstance, our scheme can realize a rather small transfer inefficiency below 1%.

### V. THE INFLUENCE OF THERMAL NOISE

The channel is not in a vacuum state in realistic setups, especially considering that usually the channel is not deeply contained inside a dilution refrigerator. For a rough estimation, we do not specify the frequency-dependence of thermal populations but simply assign a uniform distribution. Namely, we assume that every channel mode is initialized in a thermal Gibbs state that has the same average photon number denoted by  $n_{\text{th}}$ .

The results of QST inefficiency are plotted in Fig. 5. For realistic superconducting circuits, residual photon number can reach 0.01 as stated in Ref. [2]. Then Fig. 5 seems to show that thermal noise, among qubit leakage and decoherence, is the most devastating factor.

#### A. Qubits $\rightarrow$ Harmonic Resonators

However, thermal noise can be tamed by using linear setups. It has been found in Refs. [3, 4]. that the channel occupations, though affects the evolution during QST, will not change the result of QST, provided that we replace the qubits with harmonic resonators. We find the same conclusion in the multimode-resonator regime. Explicitly, we use the same sets of control pulse  $\{g_A(t), g_B(t)\}$  but assume that the qubit state has been locally written into the lowest two levels of a harmonic

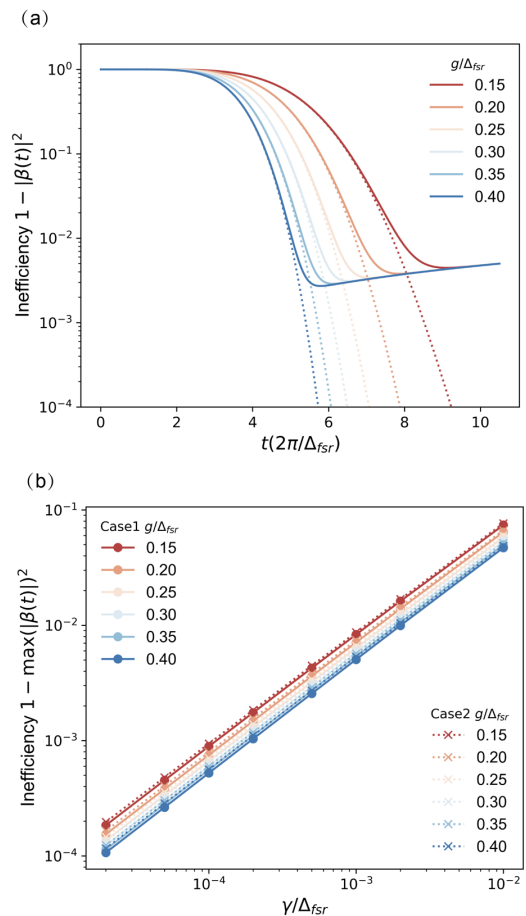


Figure 4. Numerical results considering qubit decoherence  $\gamma$ . (a) Dynamics at the receiving node. We consider Case 2 in the presence of  $\gamma/\Delta_{\text{fsr}} = 0.001$ . (b) Transfer inefficiency due to qubit decoherence  $\gamma$ .

oscillator. Now the Hamiltonian reads

$$H(t) = g_A(t)\hat{a}^\dagger \sum_k \hat{c}_k e^{-i\delta_k t} + g_B(t)\hat{b}^\dagger \sum_k (-1)^k \hat{c}_k e^{-i\delta_k t} + \text{H.c.} \quad (22)$$

where  $\hat{a}$  and  $\hat{b}$  are bosonic annihilation operators of A and B, respectively. We assume the product initial state in the form of  $|1_A, 0_B\rangle \langle 1_A, 0_B| \otimes \rho_{\text{ch}}$ , where  $\rho_{\text{ch}}$  denotes the channel state. To demonstrate that our QST scheme works for any  $\rho_{\text{ch}}$ , it is much more convenient to work in the Heisenberg picture of the above time-dependent Hamiltonian. Our target is to show that  $\hat{b}(T) = \hat{a}(0)$ , where we have assumed that QST starts at  $t = 0$  and ends at  $t = T$ .

The Heisenberg equation gives us the following equations of motion

$$\dot{\hat{a}}(t) = -ig_A(t) \sum_k e^{-i\delta_k t} \hat{c}_k(t), \quad (23)$$

$$\dot{\hat{b}}(t) = -ig_B(t) \sum_k (-1)^k e^{-i\delta_k t} \hat{c}_k(t), \quad (24)$$

where the channel mode annihilation operators can be formally written as

$$\hat{c}_k(t) = \hat{c}_k(0) - i \int_{t_i=0}^t d\tau [g_A^*(\tau) \hat{a}(\tau) + (-1)^k g_B^*(\tau) \hat{b}(\tau)] e^{i\delta_k \tau}. \quad (25)$$

These equations look similar to the Schrödinger equation of the single-excitation ansatz. But the difference is that we cannot neglect  $\hat{c}_k(0)$  as it is an operator. All the effects of the thermal populations arise from this term.

However, we notice that the linear bosonic dynamical system is “closed” in the sense that the Heisenberg picture operator  $\hat{a}(t)$ ,  $\hat{b}(t)$ , and every  $\hat{c}_k(t)$  are linear combinations of  $\hat{a}(0)$ ,  $\hat{b}(0)$  and  $\{\hat{c}_k(0)\}_k$ . This allows us to introduce the following expansions

$$\begin{aligned} \hat{a}(t) &= \alpha(t)\hat{a}(0) + \alpha_b(t)\hat{b}(0) + \sum_k \alpha_k(t)\hat{c}_k(0), \\ \hat{b}(t) &= \beta(t)\hat{a}(0) + \beta_b(t)\hat{b}(0) + \sum_k \beta_k(t)\hat{c}_k(0), \\ \hat{c}_k(t) &= c_k(t)\hat{a}(0) + c_{k,b}(t)\hat{b}(0) + \sum_j \eta_{k,j}(t)\hat{c}_j(0). \end{aligned} \quad (26)$$

Therein, the coefficients have to satisfy certain normalization restrictions. For example, the basic bosonic commutation relation  $[\hat{b}(t), \hat{b}^\dagger(t)] = 1$  implies that

$$|\beta(t)|^2 + |\beta_b(t)|^2 + \sum_k |\beta_k(t)|^2 = 1. \quad (27)$$

Therefore, the Heisenberg equations can be reduced to

the coupled equations for the coefficients of each operator at  $t = 0$ .

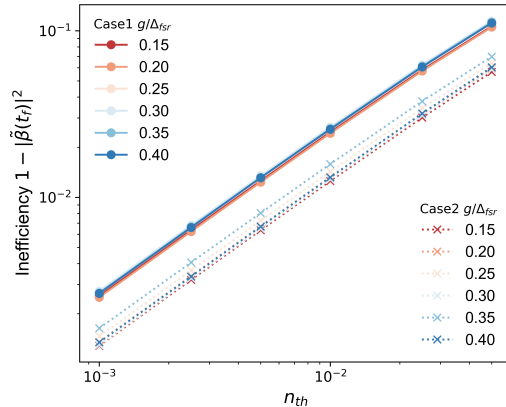


Figure 5. Transfer inefficiency due to thermal noise in the channel. The channel initial state is assumed to be a thermal Gibbs state with a uniform average photon number  $n_{\text{th}}$  in each channel.

We focus on the equations for the coefficients of  $\hat{a}(0)$ , i.e.,  $\alpha(t)$ ,  $\beta(t)$  and  $c_k(t)$ . These equations have exactly the same expression with the single-excitation Schrödinger equation. Immediately, the success of QST in the single-excitation ansatz implies the coefficients in the Heisenberg picture  $\tilde{\beta}(t_f) \approx 1$ . Then the normalization condition Eq. (27) directly gives the expected result that up to exponentially corrections,

$$\hat{b}(T) = \hat{a}(0).$$

It means that our QST scheme is immune to thermal channel population after replacing qubits with harmonic oscillators.

[1] Z. Li, P. Liu, P. Zhao, Z. Mi, H. Xu, X. Liang, T. Su, W. Sun, G. Xue, J.-N. Zhang, W. Liu, Y. Jin, and H. Yu, *npj Quantum Information* **9**, 111 (2023).  
 [2] A. Marquet, S. Dupouy, U. Réglade, A. Essig, J. Cohen, E. Albertinale, A. Bienfait, T. Peronnin, S. Jezouin, R. Lescanne, and B. Huard, *Phys. Rev. Appl.* **22**, 034053

(2024).  
 [3] B. Vermersch, P.-O. Guimond, H. Pichler, and P. Zoller, *Phys. Rev. Lett.* **118**, 133601 (2017).  
 [4] Z.-L. Xiang, M. Zhang, L. Jiang, and P. Rabl, *Phys. Rev. X* **7**, 011035 (2017).